Field, E. J., Scurr, D. J., Piggott, M. J., Anderson, T. S., & Chanoit, G. P. (2019). The chemical and ultra-structural analysis of thin plastic films used for surgical attenuation of portosystemic shunts in dogs and cats. *Research in Veterinary Science*, *126*, 192-198. https://doi.org/10.1016/j.rvsc.2019.08.023

Original Article

The chemical and ultra-structural analysis of thin plastic films used for surgical attenuation of portosystemic shunts in dogs and cats

Elinor J Field, BVetMed[a]; David J Scurr, BSc, PhD[b]; Matthew J Piggott, MPharm, PhD[b], Thomas S Anderson, BVSc[a]; Guillaume P. Chanoit, DEDV,PhD[a]*

[a] *University of Bristol, Faculty of Health and Science, School of Veterinary Sciences*
[b] *University of Nottingham, School of Pharmacy, Advanced Materials and Healthcare Technologies*

*Corresponding author Dr G Chanoit Tel:+ 44 117 394 0513

Email address g.chanoit@bristol.ac.uk (G.P. Chanoit).

Abstract

The objective of the study was to (1) characterize and compare the chemical composition at the surface, subsurface and in the bulk of thin plastic films used for portosystemic shunt attenuation in their native state and after plasma exposure. (2) Assess the presence, concentration and location of irritant compounds (e.g dicetyl phosphate) within the films.

Attenuated Total Reflectance Infrared Spectroscopy (ATR-IR), X-ray Photoelectron Spectroscopy (XPS) and dynamic Time-of-Flight Secondary Ion Mass Spectrometry (ToF-SIMS) were used to analyze thirteen thin plastic films. Sample thickness was visualized and measured using Scanning Electron Microscopy (SEM). Sample thicknesses were compared using a one-way ANOVA.

XPS reported low phosphorous concentrations (surrogate marker of dicetyl phosphate) between 0.01-0.19% wt at the sample surfaces (top 10nm). There were significant differences between film thicknesses ($P<0.001$) observed by SEM. The ATR-IR and ToF-SIMS identified four distinct surface and bulk chemical profiles: 1) Cellophane, 2) Polypropylene, 3) Modified Cellophane, and 4) Unique. Following plasma immersion for 6 weeks, samples showed little change in film thickness or chemical composition.

This study confirmed that films used to attenuate portosystemic shunts were commonly not pure cellophane, with significant variations in surface and bulk chemistry. Suspected irritant compounds were not readily identifiable in significant proportions. Pronounced variability existed in both the thickness and chemical composition of these films (surface vs. bulk). The present findings lead to a legitimate question about the reproducibility of shunt occlusion when using thin plastic films from different origins.

Keywords: portosystemic shunt; cellophane band; thin plastic film; chemistry; spectroscopy

Introduction

The use of cellophane bands for attenuation of portosystemic shunts in dogs and cats is a widely accepted method of treatment (Sereda and Adin, 2005). Various guidelines describing how to place and maintain the cellophane band around the shunt have been proposed including the recommended thickness of the band, its width, the degree of partial attenuation at the time of placement, or the number and orientation of metal clips to hold the band in place (Frankel et al., 2006; Hunt et al., 2004; McAlinden et al., 2010; Youmans and Hunt, 1998).

The attenuation process should ideally be effective, reproducible (same outcome if several surgeons use the same "cellophane band") and repeatable (e.g. same outcome if one surgeon uses different "cellophane bands"). Unfortunately, the mechanism by which "cellophane banding" induces partial or complete attenuation of the shunting vessel is poorly elucidated and thought to be related to a foreign body reaction caused by the placement of the band around the vessel. Interestingly, persistent shunting following surgery with cellophane bands has been frequently reported, with figures ranging from 18.6% to 35% of cases (Landon et al., 2008; Nelson and Nelson, 2016; Schaub et al., 2016; Matiasovic et al., 2018).

A recent study (Smith et al., 2013) looked at the mechanical and spectroscopic profile of four thin plastic films (TPF) marketed as cellophane and used clinically for portosystemic shunt attenuation in dogs and cats. Three of the four samples were not consistent with cellophane and were primarily polyester or olein fibers. It was therefore hypothesized, that the inflammatory response induced by the films was not due to the chemical composition of the film itself but instead could be due to products added during the manufacturing process. Additives agents are combined to polymer films to improve their properties and prolong their life. A common agent added during processing of these TPFs is dicetyl phosphate as a stripping agent (Laforet and

Hering, 1963; Yeager and Cowley, 1948). This agent has been shown to cause a marked inflammatory response in experimental animals and has been suggested to be responsible for inducing the inflammatory response seen with cellophane (Dahl et al., 1960; Smith et al., 2013). The determination of the presence of this agent requires the use of technique capable of assessing material characteristics at the molecular level.

Research in the field of biomaterials and surgical implants use a panel of advanced techniques for assessing material characteristics at the molecular level. Attenuated Total Reflectance Infrared Spectroscopy (ATR-IR), X-ray photoelectron spectroscopy (XPS), and Time-of-Flight Secondary Ion Mass Spectrometry (ToF-SIMS) are surface sensitive techniques, each providing different analytical depths and complementary physicochemical information.

ATR-IR and XPS techniques have been successfully applied to study several biomaterials in human and veterinary medicine (Ribuffo et al., 2015, Ameen et al., 1993, Tam et al., 2005 Elsohaby et al., 2016, Lackowski et al., 2007, Anderson et al., 2018). Alone these techniques may not be sensitive enough to define the very top surface of a material (<10nm). ToF-SIMS however has an analytical depth of a few atomic layers and can also be used dynamically (depth profiling) detecting concentrations as low as parts per billion (Belu et al., 2003).

The aim of this study was to apply advanced materials characterization techniques to investigate the chemical composition and physical state of a large number of TPF used to attenuate portosystemic shunts. This was performed with an emphasis on chemical identity, consistency, distribution (surface vs. bulk) and the relative concentration of irritant compounds such as dicetyl phosphate.

Our hypotheses were 1) there will be a significant amount of inter- and intra-film homogeneity in chemical composition and 2) irritant compounds will be consistently present either on the surface or in the bulk of the films.

Materials and Methods

Samples used for the attenuation of portosystemic shunts in dogs and cats were collected from referral institutions in Europe and North America. These were analyzed through a series of materials characterization techniques to assess the chemical composition of their surface, sub-surface and bulk. Three chemical analyses were performed on all the films in both their native state and after six weeks of plasma immersion (*The results and discussion on the latter are reported in a supplementary file)*. These were: (1) ATR-IR to assess subsurface (bulk) chemical character, (2) XPS to quantify elemental composition of the top surface and (3) ToF SIMS to provide surface to bulk chemical depth profiles. The TPF thickness of these samples was measured directly from electron micrographs collected by Scanning Electron Microscopy (SEM). Chemical composition was identified where possible by combining the techniques and referring to reference libraries (in-house and bespoke for biomaterials analysis). Additionally, two samples of each TPF were sterilized by steam and ethylene oxide treatment and compared to non-sterilized samples by traditional Fourier-transform infrared spectroscopy (FT-IR).

FT-IR -Two samples of each TPF were sterilized; one using steam (autoclaved at 121 degrees for 21 minutes) and one using ethylene oxide sterilization process. The two sterile and one non-sterile samples were tested using FTIR spectroscopy[1] at spectral window of 4-7000cm-1 – 100s

[1] Perkin Elmer Spectrum 100, PerkinElmer Life and Analytical Sciences, CT, USA

cm-1. The spectroscopic profiles between sterilized groups were compared to non-sterile samples to assess if there was any impact of the sterilization method on the chemical composition.

ATR-IR-ATR-IR spectra were recorded using a spectrophotometer with a diamond ATR module.[2] ATR-IR uses a crystal in direct contact with the surface of interest to interrogate the sample chemistry. The IR beam is totally internally reflected from the internal surface of the crystal. This generates an orthogonal evanescent wave which will project into the sample, and it is the absorption of this energy and reflected radiation that is detected. This contrasts with traditional FTIR which looks at the transmission of the IR beam through a thin (<50µm) sample section or specially prepared KBr sample disc. ATR-IR enables the analysis of 'real' samples in their native state and a focus on the surface and subsurface chemistry. Background spectra (32) were collected after crystal cleaning. Samples were then loaded onto the stage and analysed after clamping onto the crystal using the ATR module. The spectral resolution used was $2cm^{-1}$ over a spectral window of 4,000 to 650 cm^{-1}.

XPS-Samples were analyzed using an X-ray photoelectron spectrometer,[3] with a mono-chromated Al kα X-ray source (1486.6eV) operated at 10mA emission current and 12kV anode potential (120W). A wide (survey) scan and high-resolution scans were performed on each sample. The peak areas in the wide scan data were used to calculate elemental atomic percentages using Kratos relative sensitivity factors (RSFs). Data processing was carried out

[2] Agilent Cary 630 FTIR Spectrophotometer with diamond ATR module and MicroLab FTIR software v.4.0, Agilent Technologies, Cal, USA
[3] Kratos AXIS ULTRA Kratos Analytical Ltd, UK

using CASAXPS software with Kratos sensitivity factors (RSFs) to determine atomic percentage values from the peak areas.

***ToF SIMS*-** Samples were analyzed with a mass spectrometer [4] using a bismuth liquid metal primary ion gun (specifically Bi_3^+) operated at 25kV, with a single-stage reflectron analyser. Surface analysis was performed over a 500 × 500 μm area at 256 × 256 pixel resolution for 15 scans. As the samples were not conductive, charge compensation was applied in the form of a low energy (<20eV) electron floodgun and analysis was maintained in the static regime with a primary ion dose density of $< 1 \times 10^{12}$ ions/cm^2.
Depth profiling was performed using a 10 keV Ar_{1000}^+ sputter beam to etch a crater of 400 × 400μm area with analysis of the central 200 × 200μm area. Depth profiling was performed in 'non-interlaced' mode with 1 frame of analysis followed by 5s of sputter time. Data acquisition and analysis was performed using the instrument software.[5]

***SEM*-**Film samples were mounted at 90 degrees onto aluminum stubs and fixed using carbon cement. Samples were sputter coated with gold for four minutes at 24mA using a Leica EM SCD005 Sputter Coater to enable imaging at high vacuum. A scanning electron microscope[6] was used to obtain the electron micrographs. The SEM was operated in high vacuum mode at magnifications between ×940 and ×1600. Three images were taken of each film and the film

[4] ToF-SIMS IV, ION-TOF GmbH, Germany
[5] SurfaceLab 6, ION-TOF GmbH, Germany
[6] JEOL 6060LV variable pressure scanning electron microscope, JEOL Inc., Ma, USA

thickness measurements were made using the microscope-associated software[7] on two of the images from each set. Care was taken to account for the additional thickness of the gold coating.

Statistical analysis-A one-way ANOVA was performed to determine the presence of statistical differences in thickness between samples, significance was set at $P < 0.05$.

Results

Thirteen TPFs and one sample of known cellophane (control: sample 1) were collected. The control sample was collected from a bank of defined samples at the School of Chemistry, University of Bristol.

FT-IR-Following steam sterilization both colored samples (samples 12 and 13) leached their color into the sterilization packaging. However, no difference in FT-IR spectra (not shown) was seen between sterile (ethylene oxide or steam) and non-sterile samples. All subsequent analysis was performed on non-sterile samples.

ATR-IR-The ATR-IR data collected from the sample cohort demonstrated clearly that the films did not all share the same chemical character. Three broad groups of film chemistries were identified with two outliers (separated into a fourth group) as illustrated in Fig. 1 which represents the chemical "identity" of the subsurface of the bands. Group 1 was comprised of 3 samples (films 1, 2, and 10) and was identified as having spectra consistent with cellophane.

[7] JEOL's smile view software, JEOL Inc., Ma, USA

Group 2 was comprised of 5 samples (films 4, 6, 7, 9 and 13) and all showed IR spectra consistent with polypropylene.

Samples 5, 8 11 and 14 were placed into group 3 as they appeared to present ATR-IR spectra very similar to the ATR-IR data observed for the cellophane samples (group 1), however distinct variations were discerned. Variations compared to group 1 include a reduction in the intensity of both the O-H and C-O bands, and much stronger (or new) peaks at ~1650cm^{-1} and ~1280cm^{-1}. The former likely describes a distinct C-C band, with the latter a chemical state variation of a C-O group. The data suggests that these films have cellophane character but with some form of modification or variation.

Samples 3 and 12 were placed into group 4 as non-conforming samples. Sample 3 exhibited dissimilar FT-IR spectral data to all the other samples suggestive of a unique chemistry. Sample 12 had a strong FT-IR spectral relationship to the group 2 samples i.e. polypropylene chemistry. No exact chemical match was found for the films in group 4 and therefore further analysis would be recommended to expand on identification.

ToF-SIMS- The chemistry of the surface and depth of a sampled thin film from each group identified with ATR-IR is represented in Figure 2 and 3 respectively. It is in part in agreement with the observations made by the ATR-IR analysis, specifically in the identification of samples 1, 2, and 10 (group 1) as cellophane and samples 4, 6, 7, 9 and 13 (group 2) as polypropylene. Cellulose is identifiable by a series of prominent secondary ion peaks evident in their spectra, for example CHO_2^- (m/z = 44.99), $C_2H_3O_2^-$ (m/z = 59.01) and $C_3H_3O_2^-$ (m/z = 71.01) as illustrated in Fig. 2. The sample chemistry identified by surface analysis (Fig. 2) and the depth profile analysis

(Fig. 3) of this series of samples (group 1) suggests that the chemistry is entirely comprised of cellophane in accordance with the observations made by ATR-IR analysis.

The samples identified as group 2 in the ATR-IR analysis illustrate secondary ion peaks characteristic of polypropylene such as C_2H^- (m/z = 25.00) and C_4H^- (m/z = 49.00) as illustrated in Fig. 2. The depth profile data of the group 2 series of samples shows a similar chemistry throughout the profile suggesting a consistent polypropylene chemistry.

The samples identified as group 3 in the ATR-IR analysis, considered similar to cellophane, did not show the presence of secondary ions identified as being representative of cellophane in the surface analysis. The chemistry of the surface was not identified at present, however, it appeared to have a nitrogen content as identified by secondary ion peaks such as NO_2^-. At around 25s of depth profiling an interface was observed whereby the material chemistry is observed to switch to one which corresponds to cellophane (illustrated by the increase in the $C_3H_3O_2^-$ ion shown in Fig. 2). The ToF-SIMS depth profile (Fig. 3). data would suggest that these samples are cellophane in bulk with an initial unidentified layer in group 3.

The ToF-SIMS surface analysis for the final two samples (identified as group 4) also exhibited an unknown initial surface layer with a different chemistry to the bulk (Figs. 2 and 3). Sample 12 appeared to have a surface chemistry containing nitrogen before a polypropylene bulk chemistry. Sample 3 appeared to exhibit a surface layer and bulk chemistry similar to what might be anticipated from a methacrylate polymer with phosphate present within the bulk. It should also be noted that while very low intensities of various phosphate ion derivatives could be identified on all samples, these intensities were typically very low and limited to small phosphate groups.

***XPS*-**The elemental quantification of the film surfaces by XPS is shown in table 1. The films are arranged into the groups as defined above. XPS data for samples 13 and 14 was not collected due to sample availability limitations. The major elemental constituents of all the films were carbon and oxygen. Variability in total weight percentage could be seen with ranges from 51-96% atomic weight (wt) and 3-42%wt respectively. Some trace elements (sodium, calcium, silicon and nitrogen) were inconsistently identified across the sample set. Phosphorous (used as a marker for dicetyl phosphate) was detected at the surface of all films but at a consistently low level (0- 0.19%wt). Sample 11 was the only sample with a significant level of chlorine detected (~19%wt), which agrees with the suggestion via ToF-SIMS that this film was unique in possessing a chlorine containing or functionalized surface layer.

***SEM*-**The thickness between TPFs was seen to vary significantly (P<0.001), with a median of 22.0 µm (range 7.6-55.3 µm) (table 2). Notably the band thicknesses also seemed to demonstrate intra-sample variation in thickness in addition to inter-sample variation as demonstrated by some of the standard deviations.

Discussion

Our study has demonstrated stark differences in the chemistries and physical structures between the thirteen samples used by referral institutions in Europe and North America for portosystemic shunt attenuation. This is the first study providing information on the ultrastructure and chemistry of thin plastic film used for portosystemic shunt surgery in dogs and cats at the surface subsurface and bulk levels. Only two of the thirteen samples marketed as cellophane were

demonstrably cellophane throughout and consistent with our cellophane reference. Four had bulk chemistry typical of cellophane but both the ATR-IR data and, in particular, the surface specific analysis by ToF-SIMS showed surface specific modifications i.e. functionalized layers as illustrated on Figures 2 and 3. The importance of having initial layers overlying the bulk cellophane seen in the functionalized samples is unknown but may have an impact on modifying the initiation of the inflammatory reaction, especially considering the low concentration of markers for the hypothesized inflammatory compounds. Five samples were shown to be the biopolymer polypropylene, and two were chemically unique, despite sharing some traits of the other groups.

All forms of chemical analysis failed to detect a significant amount of what has been speculated as a likely trigger of the inflammatory process (dicetyl phosphate). What would have constituted a significant amount of irritant compound remains speculative. Dahl et al. used concentration of dicetyl phosphate of 5 and 10% to induce consistent fibrosis in a rat model (Dahl et al.,1960). An experimental study on dogs used 0.5 to 1 mg of pure dicetyl phosphate to induce pleurodesis (Laforet and Hering, 1963). It seems therefore unlikely that the low amount found in the TPFs could be judged significant and is more in the region of what could been be considered a contaminant of the TPF, based on the expert opinions of two of the authors (MJP, DJS). Based on these results it remains unclear if the inflammatory response following implantation could ever be considered to be a reproducible process amongst these TPFs.

The FT-IR analysis of unsterilized vs. sterilized films showed that both sterilization techniques did not change the spectra of the samples, thus indicating no induced chemical changes to the

samples. Some caution should be observed because transmission infrared spectroscopy is a bulk analytical technique and it is possible that the sterilization process may have only impacted the film surfaces. Equally two of the samples were colored and when steam sterilized, the dye leached around the sample. The significance of this is unclear but it could be hypothesized that there is the capacity for coloring to leach when used in a clinical setting and the effect of this should be considered. However, broadly our initial data supplements that of Smith et al (Smith et al., 2013) to recommend steam sterilization for films used in portosystemic shunt surgery.

The choice of analytical methods was based on the thickness of samples and the suspected concentrations of compounds within the samples. Thickness of samples was documented from previous studies (Smith et al., 2013) and SEM was deemed the most appropriate technique to measure sample thickness. A preliminary (data not included) study using inductively coupled plasma analysis was performed to assess the relative concentrations of phosphorous that were likely to be in the TPFs. Based on these results, it was deemed that subsequent analysis was performed with the combination of XPS, ATR-IR, and ToF-SIMS.

The present study actively shows pronounced heterogeneity in the chemistry of the bands studied and therefore, the findings lead to legitimate questions about the reproducibility of portosystemic shunt attenuation when using different films. It is likely that initial landmark papers into the use of "cellophane bands" for portosystemic shunt attenuation (Frankel et al., 2006; Hunt et al., 2004; Youmans and Hunt, 1998) did not use similar samples (the information is not available for some of these studies) and whether they were based on cellophane or another TPF. Based on the

results of our study, it seems therefore likely that the chemical and ultra-structural compositions of these bands were different, making the recommendations from these papers valid only if the same band was used. Therefore, it seems prudent to consider that outcomes for individual institutions can only be based on in-house audits and not extrapolated from published studies. It could be of particular importance when one considers that statements extracted from peer reviewed clinical studies regarding the manipulation of these bands in surgery, and logically endorsed by the majority of surgeons. For example, placement of the "cellophane band" under no tension around the abnormal vessel or folding the "band" three times before implantation are based on studies performed with different type of "bands".

This inter-band variation is likely to remain within the veterinary community, if the conception that any TPF used for shunt occlusion is "equivalent". We suggest that the selection of TPFs needs greater standardization to support reliability in the occlusion of portosystemic shunts in a clinical setting.

Conflict of Interest statement

The authors have no conflict of interest to declare.

Acknowledgements

This study was funded in part by the Langford Veterinary Services Clinical Research funds. The authors declare that there were no conflicts of interest. The authors thank Dr. Christine Whiting, Mr. Nicholas Hunt (Bristol) and Dr. Karen Alvey (Nottingham) for technical assistance.

References

Anderson, T.S., Rance, G., Jiang, L., Piggot, M., Field, E., Chanoit, G., 2018. Changes in chemical and ultrastructural composition of ameroid constrictors following in vitro expansion. PLoS One, 15;13 (11)

Ameen, A.P., Short, R.D., Johns, R., Schwach, G., 1993. The surface analysis of implant materials. 1. The surface composition of a titanium dental implant material. Clin Oral Implants Res 4, 144-150.

Belu, A.M., Graham, D.J., Castner, D.G., 2003. Time-of-flight secondary ion mass spectrometry: techniques and applications for the characterization of biomaterial surfaces. Biomaterials 24, 3635-3653.

Cabassu, J., Seim, H.B., 3rd, MacPhail, C.M., Monnet, E., 2011. Outcomes of cats undergoing surgical attenuation of congenital extrahepatic portosystemic shunts through cellophane banding: 9 cases (2000-2007). J Am Vet Med Assoc 238, 89-93.

Cowley, R.A., Yeager, G.H., 1953. Treatment of aneurysms with follow-up studies on dicetyl phosphate; a report of thirty-six cases. Surgery 34, 1032-1042.

Dahl, A.W., Fletcher, T.L., Skinner, H.H., Jr., Merendino, K.A., 1960. Fibrosing properties, in the rat, of compounds related to dicetyl (DI-n-hexadecyl) phosphate-I. Biochem Pharmacol 5, 231-237.

Elsohaby, I., McClure, J.T., Riley, C.B., Shaw, R.A., Keefe, G.P., 2016. Quantification of bovine immunoglobulin G using transmission and attenuated total reflectance infrared spectroscopy. J Vet Diagn Invest 28, 30-37.

Frankel, D., Seim, H., MacPhail, C., Monnet, E., 2006. Evaluation of cellophane banding with and without intraoperative attenuation for treatment of congenital extrahepatic portosystemic shunts in dogs. J Am Vet Med Assoc 228, 1355-1360.

Freeman, R.H., Davis, J.O., Watkins, B.E., 1977. Development of chronic perinephritic hypertension in dogs without volume expansion. Am J Physiol 233, F278-281.

Hunt, G.B., Kummeling, A., Tisdall, P.L., Marchevsky, A.M., Liptak, J.M., Youmans, K.R., Goldsmid, S.E., Beck, J.A., 2004. Outcomes of cellophane banding for congenital portosystemic shunts in 106 dogs and 5 cats. Vet Surg 33, 25-31.

Kimberlin, W.W., Wardlaw, J.L., Madsen, R.W., 2016. Effects of repeated gas sterilization on closure rates of ameroid ring constrictors in vitro. Am J Vet Res 77, 84-87.

Lackowski, W.M., Vasilyeva, Y.B., Crooks, R.M., Kerwin, S.C., Hulse, D.A., 2007. Microchemical and surface evaluation of canine tibial plateau leveling osteotomy plates. Am J Vet Res 68, 908-916.

Laforet, E.G., Hering, A.C., 1963. Intrapleural Insufflation of Dicetyl Phosphate to Promote Pleural Symphysis. Dis Chest 44, 505-508.

Landon, B.P., Abraham, L.A., Charles, J.A., 2008. Use of transcolonic portal scintigraphy to evaluate efficacy of cellophane banding of congenital extrahepatic portosystemic shunts in 16 dogs. Aust Vet J 86, 169-179.

McAlinden, A.B., Buckley, C.T., Kirby, B.M., 2010. Biomechanical evaluation of different numbers, sizes and placement configurations of ligaclips required to secure cellophane bands. Vet Surg 39, 59-64.

McKeever, D.C., 1943. The use of cellophane as an interpostion membrane in synovectomy. Journal of Bone and Joint Surgery 25, 576-580.

Matiasovic M, Chanoit G, Meakin L, Tivers M. 2018. Retrospective evaluation of surgical treatment for congenital extrahepatic portosystemic shunts by thin film banding versus ameroid constrictor placement in dogs submitted Vet Surg.

Monnet, E., Rosenberg, A., 2005. Effect of protein concentration on rate of closure of ameroid constrictors in vitro. Am J Vet Res 66, 1337-1340.

Nelson, N.C., Nelson, L.L., 2016. Imaging and Clinical Outcomes in 20 Dogs Treated with Thin Film Banding for Extrahepatic Portosystemic Shunts. Vet Surg 45, 736-745.

Page, I.H., 1939. A Method for Producing Persistent Hypertension by Cellophane. Science 89, 273-274.

Ribuffo, D., Lo Torto, F., Giannitelli, S.M., Urbini, M., Tortora, L., Mozetic, P., Trombetta, M., Basoli, F., Licoccia, S., Tombolini, V., Cassese, R., Scuderi, N., Rainer, A., 2015. The effect of post-mastectomy radiation therapy on breast implants: Unveiling biomaterial alterations with potential implications on capsular contracture. Mater Sci Eng C Mater Biol Appl 57, 338-343.

Schaub, S., Hartmann, A., Schwarz, T., Kemper, K., Pueckler, K.H., Schneider, M.A., 2016. Comparison of contrast-enhanced multidetector computed tomography angiography and splenoportography for the evaluation of portosystemic-shunt occlusion after cellophane banding in dogs. BMC Vet Res 12, 283.

Schonwalder, S.M., Bally, F., Heinke, L., Azucena, C., Bulut, O.D., Heissler, S., Kirschhofer, F., Gebauer, T.P., Neffe, A.T., Lendlein, A., Brenner-Weiss, G., Lahann, J., Welle, A., Overhage, J., Woll, C., 2014. Interaction of human plasma proteins with thin gelatin-based hydrogel films: a QCM-D and ToF-SIMS study. Biomacromolecules 15, 2398-2406.

Sereda, C.W., Adin, C.A., 2005. Methods of gradual vascular occlusion and their applications in treatment of congenital portosystemic shunts in dogs: a review. Vet Surg 34, 83-91.

Smith, R.R., Hunt, G.B., Garcia-Nolen, T.C., Stump, S., Stover, S.M., 2013. Spectroscopic and mechanical evaluation of thin film commonly used for banding congenital portosystemic shunts in dogs. Vet Surg 42, 478-487.

Tam, S.K., Dusseault, J., Polizu, S., Menard, M., Halle, J.P., Yahia, L., 2005. Physicochemical model of alginate-poly-L-lysine microcapsules defined at the micrometric/nanometric scale using ATR-FTIR, XPS, and ToF-SIMS. Biomaterials 26, 6950-6961.

Yeager, G.H., Cowley, R.A., 1948. Studies on the Use of Polythene as a Fibrous Tissue Stimulant. Ann Surg 128, 509-519.

Youmans, K.R., Hunt, G.B., 1998. Cellophane banding for the gradual attenuation of single extrahepatic portosystemic shunts in eleven dogs. Aust Vet J 76, 531-537.

Youmans, K.R., Hunt, G.B., 1999. Experimental evaluation of four methods of progressive venous attenuation in dogs. Vet Surg 28, 38-47.

Table 1

Group	Sample	Carbon (1s)%	Oxygen (1s)%	Chlorine (2p)%	Nitrogen (1s)%	Sodium (KLL)%	Calcium (2p)%	Phosphorous (2p)%	Sulphur (2p)%	Silicon (2p)%
1	1	73.62	25.28	0.00	0.00	0.13	0.25	0.00	0.12	0.60
	2	82.17	15.69	0.00	0.00	0.07	1.33	0.01	0.00	0.77
	10	50.89	41.66	0.00	0.25	0.00	0.00	0.02	0.00	7.19
2	4	80.18	18.24	0.00	0.00	0.15	0.04	0.01	0.00	1.38
	6	71.52	23.37	0.00	4.79	0.02	0.05	0.03	0.00	0.27
	7	95.66	3.19	0.00	0.00	0.37	0.21	0.05	0.05	0.47
	9	63.84	29.47	0.00	5.85	0.00	0.08	0.05	0.00	0.74
3	5	90.91	7.35	0.00	0.00	0.42	0.10	0.03	0.00	1.19
	8	96.89	3.00	0.00	0.00	0.00	0.05	0.06	0.00	0.00
	11	75.00	5.73	18.87	0.00	0.08	0.00	0.19	0.01	0.24
4	3	83.55	14.69	0.00	0.72	0.42	0.09	0.02	0.00	0.50
	12	89.52	7.46	0.08	0.68	0.42	0.52	0.05	0.06	1.20

8

Table 2

Sample	Mean thickness	
	µm	SD
1 (pure cellophane)	**36.8**	**0.98**
2	25.1	1.81
3	7.6	1.06
4	20.1	1.83
5	21.4	1.54
6	34.5	9.60
7	45.4	4.84
8	19.7	1.62
9	55.3	18.33
10	18.1	0.72
11	27.2	0.95
12	22.5	2.37
13	19.4	1.30
14	20.6	1.40

X-ray photoelectron spectroscopy (XPS) analysis showing the % weight of the detected elements within each thin plastic film group. Due to limitations on sample availability no XPS data is available for samples 13 and 14. Sample 1 is the control sample (pure cellophane).

9

Figure Legends

Fig. 1. ATR-IR spectra of the Thin Plastic Films (TPFs) pre-plasma immersion. The TPFs are divided into 4 groups: 1) Cellophane, 2) Poly-propylene, 3) Modified Cellophane, 4) Unique. In group 1: A strong and broad O-H stretching band can be seen from approximately 3600-3100cm^{-1}, with a C-H stretching band at around 2900cm-1, as well as an additional characteristic sequence of bands in the 1500-800 cm^{-1} spectral region. These include a strong C-O stretch (1040 cm^{-1}) and both C-H and C-H_2 bending (1380, 1400 cm^{-1}).
In group 2, these spectra were characterized by strong CH_3 stretches at 2970 cm^{-1} and 2910 cm^{-1}, CH2 stretches at 2870 cm^{-1} and 2840 cm^{-1}, a CH_2 bend at 1460 cm^{-1} and a CH_3 stretch at 1370 cm^{-1}. Group 3 samples show a very similar profile to the group 1 traces but with a suppressed O-

[9] Scanning electron microscopy thickness of samples pre and post plasma immersion. Sample 1 is the control sample (pure cellophane) - SD: Standard Deviation

H stretching band, variations on the CH stretching bands and additional peaks in the fingerprint region (1500 cm^{-1} - 500cm^{-1}). Group 4 samples show sufficiently different chemical character to be considered unique.

Fig. 2. Time-of-Flight Secondary Ion Mass Spectrometry surface spectra from a representative sample from each of the group (pre-plasma immersion).

Fig. 3. Time-of-Flight Secondary Ion Mass Spectrometry depth profile from a representative sample from each of the group (pre-plasma immersion).

Plasma immersion study

Material and methods

A sample of each non-sterile TPF was placed in a Petri dish with 60mls of canine plasma[1]. The plasma was mixed with penicillin (100 U/ml), streptomycin (100 mg/ml) and amphotericin B (2.5mg/ml) to minimize growth of bacterial and fungal contaminants. The samples were incubated at 38 C for six weeks. The samples were then removed from the plasma, washed with saline before the ATR-IR, ToF-SIMS and SEM were repeated. XPS (a surface specific technique) was not performed due to the likelihood of post plasma samples being surface contaminated (due to long standing immersion in Petri dishes). The protein concentration was measured, and the plasma was cultured.

Results

***Plasma analysis*-**The plasma was analyzed post TPF immersion and the total protein concentration was 12.9 g/dL, albumin concentration was 5.0 g/dL and globulin concentration was 7.9g/dL. Positive culture results were obtained from two samples (3 and 12). Considering there was no change in these samples' chemical structure, these samples were not excluded.

***Spectroscopic analysis*-**Following plasma immersion ToF-SIMS surface analysis and depth profiling were used to analyze the TPFs. ToF-SIMS data was very similar to that from the pre-immersion samples. Some subtle differences were seen such as the group 1 films presenting with

[1] Petblood bank,UK

an additional superficial layer of CN-rich chemistry at the top surface. The sample within group 3 which already had an initial chloride surface layer (sample 11) showed an increase in intensity of this ion, possibly indicating that chlorine had leached into / onto the sample from the plasma treatment or saline wash. Group 3 overall had similar findings to group 1, although in these samples there was a heightened incidence of the chloride ion, but restricted to the top surface. In Group 2 there was very little change in chemical structure and although present, far less adherence of any nitrogen rich chemistries. The two unique films in group 4 did again show an adhesion of CN containing chemistries to the top surface. Overall, there was negligible change in the chemical composition of the TPFs, especially in relation to subsurface and bulk composition. However, Groups 1 and 3 did appear to take up chloride ions from the treatment process whereas the other groups did not. All samples had an additional nitrogen rich surface layer, which is likely adherence of components of the plasma to the samples.

TPFs were also analyzed by ATR-IR. Data showed an almost complete consistency with the initial data. As the films were unlikely to degrade substantially in these conditions and timeframes, any induced differences were likely to be surface specific (absorption etc.) and therefore it is not unsurprising that the ATR-IR data was not sensitive to this.

Following plasma immersion, there was a significant increase in film thickness in samples 1,3,4,6,10,13 and a significant decrease in samples 2, 5,9,11. Samples 7,8,12 and 14 showed no significant change in thickness. The median band thickness following plasma immersion was 23.11 µm (range 15.48-53.0µm) (see table S1 and Fig. S1)

Discussion

The rate of elution of chemical compounds from the film is very difficult to measure *in vitro*. We immersed samples in plasma, at 38°C for six weeks to try and mimic the environment the samples are exposed to *in vivo*. The period of six weeks of incubation was arbitrarily decided and is accordance with the time period used in previous experimental studies on "cellophane bands" (Youmans and Hunt, 1999). This is significantly longer than the incubation time used in recent *in vitro* studies on ameroid constrictor, (Kimberlin et al., 2016) which may explain why two of the 14 samples were contaminated despite the use of the same antibacterial and antifungal protocol. Protein concentration in our samples was over twice the concentration inducing the maximum effect on the rate of closure of ameroid ring constrictor (Monnet and Rosenberg, 2005). It was therefore hypothesized that if protein concentration had any effect on the structure of the TPFs it would be evidenced with such high concentrations.

The analyses on the samples post plasma treatment showed very little difference in the physical or chemical structures. It is expected that the samples are exposed to other factors *in vivo* rather than just tissue fluid, that incite the inflammatory response, most pertinent being the immune system cells. However, if the sample surfaces are not showing a marked change in structure post plasma immersion (dissolution, roughening) then it is likely that the most important factor for influencing the inflammatory response will remain the chemistry of the surface layer in contact with the blood vessel. This highlights the potential importance of surface layers over a bulk.

Figure legends

Table S1-Scanning electron microscopy thickness of samples pre and post plasma immersion.

Sample 1 is the control sample (pure cellophane)

Sample	Mean thickness Pre plasma		Mean thickness Post plasma	
	µm	SD	µm	SD
1 (pure cellophane)	**36.8**	**0.98**	**53.0**	**2.40**
2	25.1	1.81	15.48	1.19
3	7.6	1.06	16.52	2.50
4	20.1	1.83	24.64	0.55
5	21.4	1.54	17.14	0.61
6	34.5	9.60	46.28	1.29
7	45.4	4.84	45.44	0.63
8	19.7	1.62	19.36	1.19
9	55.3	18.33	48.0	1.21
10	18.1	0.72	20.32	0.19
11	27.2	0.95	24.86	1.41
12	22.5	2.37	22.6	0.93
13	19.4	1.30	23.62	0.25
14	20.6	1.40	21.92	0.30

SD: Standard Deviation

Fig.S1: Thin plastic film thickness before and after plasma exposure. *X*-axis represents the sample and *y*-axis represents the thickness in µm

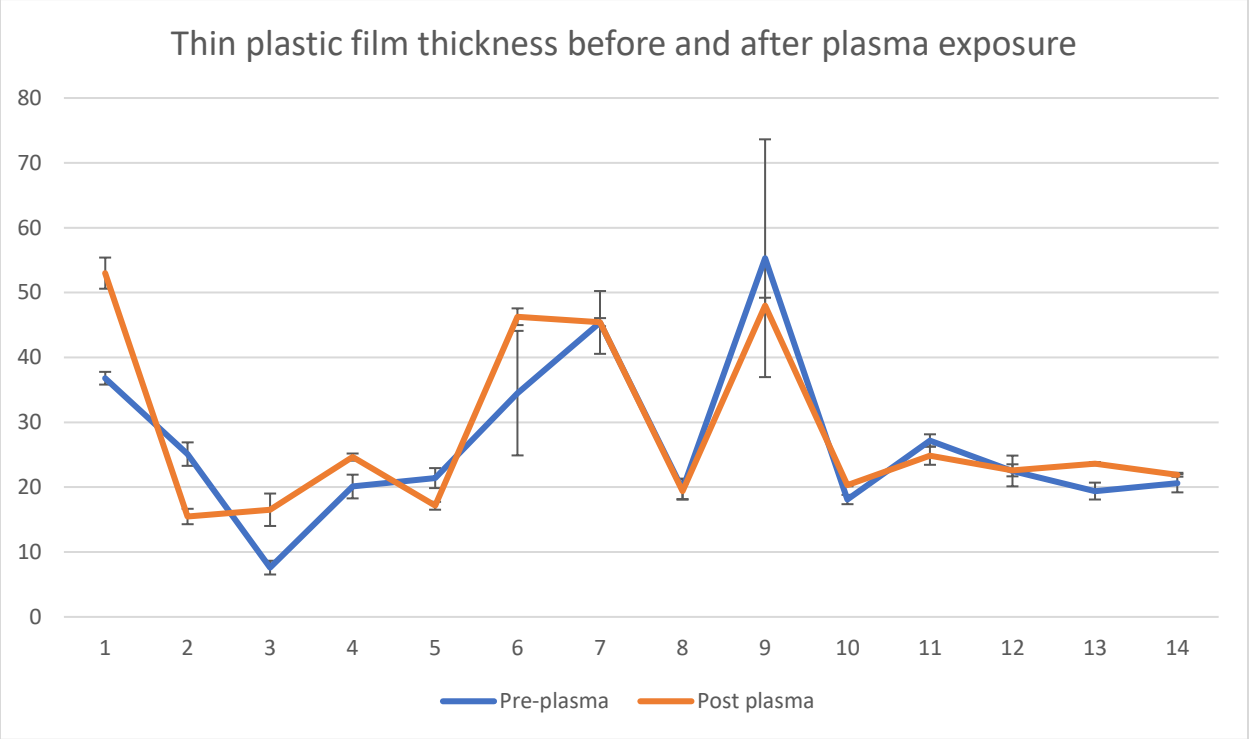

Group	Sample	Carbon (1s) %	Oxygen (1s) %	Chlorine (2p) %	Nitrogen (1s) %	Sodium (KLL) %	Calcium (2p) %	Phosphorous (2p) %	Sulphur (2p) %	Silicon (2p) %
1	1	73.62	25.28	0.00	0.00	0.13	0.25	0.00	0.12	0.60
	2	82.17	15.69	0.00	0.00	0.07	1.33	0.01	0.00	0.77
	10	50.89	41.66	0.00	0.25	0.00	0.00	0.02	0.00	7.19
2	4	80.18	18.24	0.00	0.00	0.15	0.04	0.01	0.00	1.38
	6	71.52	23.37	0.00	4.79	0.02	0.05	0.03	0.00	0.27
	7	95.66	3.19	0.00	0.00	0.37	0.21	0.05	0.05	0.47
	9	63.84	29.47	0.00	5.85	0.00	0.08	0.05	0.00	0.74
3	5	90.91	7.35	0.00	0.00	0.42	0.10	0.03	0.00	1.19
	8	96.89	3.00	0.00	0.00	0.00	0.05	0.06	0.00	0.00
	11	75.00	5.73	18.87	0.00	0.08	0.00	0.19	0.01	0.24
4	3	83.55	14.69	0.00	0.72	0.42	0.09	0.02	0.00	0.50
	12	89.52	7.46	0.08	0.68	0.42	0.52	0.05	0.06	1.20